Synthesis and Magnetic Properties of Six New Trinuclear Oxo-Centered Manganese Complexes of General Formula $[Mn_3O(X\text{-benzoato})_6L_3]$ (X = 2-F, 2-Cl, 2-Br, 3-F, 3-Cl, 3-Br; L = Pyridine or Water) and Crystal Structures of the 2-F, 3-Cl, and 3-Br Complexes

Joan Ribas,*[1a] Belen Albela,[1a] Helen Stoeckli-Evans,[1b] and George Christou[1c]

Departament de Química Inorgànica, Universitat de Barcelona, Diagonal, 647, 08028-Barcelona, Spain, Institut de Chimie, Université de Neuchâtel, Avenue de Bellevaux 51, CH-2000 Neuchâtel, Switzerland, and Department of Chemistry, Indiana University, Bloomington, Indiana 47405-4001

Received October 18, 1996[⊗]

The reaction of N-*n*-Bu_4MnO_4 or $NaMnO_4$ with appropriate reagents in ethanol−pyridine leads to the high-yield formation of new mixed-valence trinuclear oxo-centered $Mn^{III,III,II}$ complexes of general formulation $[Mn_3O(X\text{-benzoato})_6L_3]$ (**1**, X = 2-fluoro, L = pyridine; **2**, X = 2-chloro, L = pyridine; **3**, X = 2-bromo, L = pyridine; **4**, X = 3-fluoro, L = 2 pyridine + 1 H_2O; **5**, X = 3-chloro, L = 2 pyridine + 1 H_2O; **6**, X = 3-bromo, L = 2 pyridine + 1 H_2O). The crystal structures of **1**, **5**, and **6** were determined. Complex **1** crystallizes in the monoclinic system, space group $C2/c$ with $a = 15.774(2)$ Å, $b = 17.269(2)$ Å, $c = 21.411(2)$ Å, $\beta = 91.11(1)°$, and $Z = 4$. Complex **5** crystallizes in the monoclinic system, space group $P2_1/n$ with $a = 15.172(2)$ Å, $b = 17.603(2)$ Å, $c = 21.996(3)$ Å, $\beta = 106.300(10)$, and $Z = 4$. Complex **6** crystallizes in the monoclinic system, space group $P2_1/n$ with $a = 15.533(3)$ Å, $b = 17.884(2)$ Å, $c = 21.997(4)$ Å, $\beta = 106.95(1)°$, and $Z = 4$. The three complexes are neutral and possess an oxo-centered Mn_3O unit with peripheral ligands provided by bridging carboxylate and terminal pyridine or H_2O groups. Each manganese ion is distorted octahedral, and consideration of overall charge necessitates a mixed-valence $Mn^{II}Mn^{III}_2$ description. In **1,** the presence of a C_2 axis through the central O atom and one of the manganese atoms (Mn^{II}) and the absence of imposed symmetry elements in **5** and **6** (they have the two Mn^{III} with a terminal pyridine group and the Mn^{II} with a H_2O terminal molecule) suggest a trapped-valence situation in all three cases. The Mn^{II} is assigned on the basis of its longer metal−ligand distances. Variable-temperature magnetic susceptibility studies were performed on **1**−**6** in the temperature range 2−300 K. Satisfactory fits to the observed susceptibility data were obtained by assuming isotropic magnetic exchange interactions and using the appropriate spin Hamiltonian and susceptibility equation. The derived J and J^* exchange parameters are all relatively small in magnitude, $|J| < 10$ cm^{-1}. J characterizes the $Mn^{II}\cdots Mn^{III}$ interactions and J^* the $Mn^{III}\cdots Mn^{III}$ interaction. Magnetization measurements at 2 K up to 50 kG indicate the variability of the ground state: $S = {}^3/_2$ for **2** and **3**; $S = {}^1/_2$ for **1**, **4**, and **5**; and $S = {}^3/_2$, ${}^1/_2$ for **6**. X-band EPR spectra measured from 4 K to room temperature on polycrystalline samples of **1**−**6** show highly significant differences when the ground state is ${}^3/_2$ or ${}^1/_2$. For $S = {}^3/_2$ complexes (**2** and **3**), there is a transition centered at $g \approx 4$, which decreases in intensity with increasing temperature. For $S = {}^1/_2$ complexes, this $g \approx 4$ band does not appear but instead there are broad bands centered at $g \approx 2$. These results are discussed in terms of spin frustration within the Mn_3O core, which produces different spin ground states and susceptibility values.

Introduction

A recent study of the ground-state variability in μ_3-oxide trinuclear mixed-valence manganese complexes has been carried out by McCusker *et al*.[2] This study is based on the comparison between $[Mn_3O(acetato)_6(pyr)_3]$ and $[Mn_3O(benzoato)_6(pyr)_2(H_2O)]$. The former has a ground state of ${}^3/_2$ whereas the ground state of the latter is ${}^1/_2$. In fact, the ground state of a $Mn^{II}Mn^{III}_2$ complex can range from $S = {}^1/_2$ to $S = {}^{13}/_2$, depending on the spin frustration.[3] By varying the ratio of the J and J^* exchange parameters in a $Mn^{II}Mn^{III}_2$ complex, without making large changes in these parameters, it is possible to stabilize a ground state with $S \neq {}^1/_2$. Unfortunately, the number of $Mn^{II}Mn^{III}_2O$ complexes has been the object of only limited investigation to date. The first reported structures of these complexes were the $[Mn_3O(acetato)_6(pyr)_3]pyr$[4] and $[Mn_3O(acetato)_6(3Cl\text{-}pyr)_3]$.[5] Later, in 1987, Vincent *et al*. reported the synthesis, characterization and crystal structure of $[Mn_3O(acetato)_6(pyr)_3]$-pyr and $[Mn_3O(benzoato)_6(pyr)_2(H_2O)]0.5MeCN$.[6] Several other complexes with the same characteristics but lacking crystal structure were presented in ref 6; one of them has the imidazole ligand instead of pyridine linked to manganese ions. The crystal structure of a very similar trinuclear complex with benzoato as bridging ligand but with three pyridines as terminal ligands has recently been reported[7] without magnetic studies. The crystal structure of a new trinuclear complex with pivalic acid, $[Mn_3O$-

⊗ Abstract published in *Advance ACS Abstracts,* May 1, 1997.

(1) (a) Departament de Química Inorgànica, Universitat de Barcelona, Diagonal 647, 08028-Barcelona, Spain. (b) Institut de Chimie, Université de Neuchâtel, Avenue de Bellevaux 51, CH-2000 Neuchâtel, Switzerland. (c) Department of Chemistry, Indiana University, Bloomington, IN 47405-4001.

(2) McCusker, J. K.; Jang, H. G.; Wang, S.; Christou, G.; Hendrickson, D. N. *Inorg. Chem.* **1992**, *31*, 1874.

(3) McCusker, J. K.; Schmitt, E. A.; Hendrickson, D. N. High Spin Inorganic Clusters: Spin Frustration in Polynuclear Iron and Manganese Complexes. In *Magnetic Molecular Materials*; Gatteschi, D., Kahn, O., Miller, J. S., Palacio, F., Eds.: Kluwer Academic Publisher: Dordrecht, The Netherlands, 1991; pp 297−319.

(4) Baikie, A. R. E.; Hursthouse, M. B.; New, D. B.; Thornton, P. *J. Chem. Soc., Chem. Commun.* **1978**, 62.

(5) Baikie, A. R. E.; Hursthouse, M. B.; New, L.; Thornton, P.; White, R. C. *J. Chem. Soc., Chem. Commun*. **1980**, 684.

(6) Vincent, J. B.; Chang, H. R.; Folting, K.; Huffman, J. C.; Christou, G.; Hendrickson, D. N. *J. Am. Chem. Soc*. **1987,** *109*, 5703.

(7) Hao, X.; Jin-Yu, L.; Qi, L.; Zheng, X.; Xiao-Zeng, Y.; Kai-Bei, Y. *J. Struct. Chem.* **1994,** *13*, 272.

S0020-1669(96)01252-9 CCC: $14.00

$(pivalic)_6(pyr)_3]$, has also been reported,[8] and more recently, a preliminary communication of a possible molecular ferromagnet with $T_c = 3.3$ K and $S = {}^9/_2$, $[Mn_3O(Pr^iCOO)_6(Im)_3]\cdot 3Pr^iCOOH$ was published.[9] All these compounds appear to be valence-trapped mixed-valence complexes. Nakano *et al*. and Jang *et al*. have shown that resonance exchange interactions (electron-transfer integral, *t*), typical for electronic delocalization are probably not present in these kinds of complex.[10,11] Perhaps the most striking feature in these complexes, as commented above, is the variability of the ground state, due to small changes in the structure of the trinuclear complexes.[2] In all complexes (trinuclear, tetranuclear, etc.) very subtle changes in the magnitude ratios of competing exchange interactions can have strong effects on the exact nature of ground and low-lying magnetic states.[2] The purpose of the present paper is to further our understanding of these states by preparing new trinuclear mixed-valence complexes, starting from halobenzoic acids instead of benzoic acid. These halobenzoic acids have different pK_a values: for example, the 2-fluoro is a very strong acid whereas the 3-chloro and 3-bromo are similar to benzoic acid. Here the results are presented of this synthetic work for six new complexes (with 2-fluoro- (**1**), 2-chloro- (**2**), 2-bromo- (**3**), 3-fluoro- (**4**), 3-chloro- (**5**), and 3-bromobenzoato (**6**)) together with single-crystal X-ray structures of three of these mixed-valence Mn_3O complexes (with 2-fluoro- (**1**), 3-chloro- (**5**), and 3-bromobenzoic acids (**6**)).

Experimental Section

Materials. Manganese(II) acetate, X-benzoic acids, $NaMnO_4$, and pyridine were purchased from Aldrich and used without purification. The N-*n*-Bu_4MnO_4 was prepared according to literature data.[12] The solvents MeCN, CH_2Cl_2, absolute EtOH, hexanes, and ether were used as received (Fluka, Puriss p.a. ACS >99.5%).

Synthesis. In our first attempts, the six new complexes were prepared following the method described by Vincent *et al*. for the benzoato analog:[6] $Mn(OOCMe)_2\cdot 4H_2O$ (2.00 g, 8.15 mmol) and X-benzoic acid (61.4 mmol; 8.6 g for X = F, 9.61 g for X = Cl, and 12.34 g for X = Br) were dissolved in pyridine (3 mL) and absolute EtOH (20 mL), and solid N-*n*-Bu_4MnO_4 (1.14 g, 3.15 mmol) was added in small portions and stirred to give a brown-green homogeneous solution from which begins almost immediately the precipitation of a brown-green product. The stirring was maintained for 1 h, and the new product was left undisturbed for one night in a refrigerator. The resulting brown-green precipitate was filtered, washed with cold ethanol and ether and dried in vacuo. This method gives a high yield of **1** (2-F) (85%), **2** (2-Cl) (79%), **3** (2-Br) (95%), and **4** (3-F) (75%), but not of **5** (3-Cl) and **6** (3-Br). In the latter two cases, when the N-*n*-$BuMnO_4$ was added in small portions, a new complex was formed, which nevertheless redissolved when about half the permanganate had been added, and a new red-brown solid appeared. The analysis of these new products did not correspond to any pure product. So in these two cases, the ratio of the reagents was changed, following the stoichiometric ratio of MnO_4^- and Mn^{II} according to the general equation

$$13Mn^{2+} + 2MnO_4^- + 6H^+ \rightarrow 5[Mn_3O]^{6+} + 3H_2O \qquad (1)$$

Thus, only 1.25 mmol of MnO_4^- (stoichiometric quantity required for this reaction with 8.15 mmol of manganese(II) acetate) was added instead of 3.15 mmol. Under these conditions the new complexes **5** (91%) and **6** (88%) were synthesized as above. Finally, the synthesis of **1**−**4** with this stoichiometric ratio was repeated and the complexes were also obtained in similar yield (91% for **1**; 85% for **2**, 89% for **3**, and 83% for **4**). In all cases, $NaMnO_4$ was also used instead of N-*n*-Bu_4MnO_4 with similar results. **Caution**: *This last reaction is highly energetic.* The six new complexes were found to be fairly soluble in CH_2Cl_2 and MeCN. When recrystallization was carried out in CH_2Cl_2, the method consisted of layering a concentrated solution in CH_2Cl_2 with hexanes; after several days small microcrystals of the desired product were obtained, filtered, washed with ethanol and ether, and air-dried. When recrystallization was carried out in MeCN, there were two methods: layering with ether or leaving the MeCN solution to stand for several days in the open air. Small microcrystals were obtained and treated as above. Anal. Calcd for (**1**) (in MeCN) $[Mn_3O(2F\text{-benzoato})_6(pyr)_3]CH_3CN$ ($C_{59}H_{42}F_6Mn_3N_4O_{13}$): C, 54.75; H, 3.25; N, 4.33; F, 8.81; Mn, 12.76. Found: C, 54.6; H, 3.1; N, 4.2; F, 8.8; Mn, 12.6. Anal. Calcd for (**2**) (in MeCN), $[Mn_3O(2Cl\text{-benzoato})_6(pyr)_3]$ ($C_{57}H_{39}Cl_6Mn_3N_3O_{13}$): C, 50.66, H, 2.90; N, 3.11; Cl, 15.74; Mn, 12.21. Found: C, 50.8; H, 2.9; N, 3.2; Cl, 15.8; Mn, 12.3. Anal. Calcd for (**3**) (in MeCN), $[Mn_3O(2Br\text{-benzoato})_6(pyr)_3]$ ($C_{57}H_{39}Br_6Mn_3N_3O_{13}$): C, 42.31; H, 2.43; N, 2.60; Br, 29.63; Mn, 10.20. Found: C, 42.1; H, 2.4; N, 2.7; Br, 29.7; Mn, 10.2. Anal. Calcd for (**4**) (in CH_2Cl_2) $[Mn_3O(3F\text{-benzoato})_6(pyr)_2(H_2O)]$ ($C_{52}H_{36}F_6Mn_3N_2O_{14}$): C, 52.41; H, 3.04; N, 2.35; F, 9.57; Mn, 13.85. Found: C, 52.8; H, 3.0; N, 2.5; F, 9.6; Mn, 14.0. Anal. Calcd for (**5**) (in CH_2Cl_2) $[Mn_3O(3Cl\text{-benzoato})_6(pyr)_2(H_2O)]\cdot {}^1/_2H_2O$ ($C_{52}H_{37}Cl_6Mn_3N_2O_{14.5}$): C, 47.98; H, 2.84; N, 2.15; Cl, 16.38: Mn, 12.70. Found: C, 48.0; H, 2.9; N, 2.1; Cl, 16.4; Mn, 12.7. Anal. Calcd for (**6**) (in CH_2Cl_2) $[Mn_3O(3Br\text{-benzoato})_6(pyr)_2(H_2O)]\cdot {}^1/_4H_2O$ ($C_{52}H_{36.5}Br_6Mn_3N_2O_{14.25}$): C, 39.96; H, 2.33; N, 1.79; Br, 30.72; Mn, 10.57. Found: C, 41.0; H, 2.4; N, 1.8; Br, 30.6; Mn, 10.4. With the layering methods (in the solvents indicated above) well-formed single crystals of **1**, **5**, and **6** were obtained.

IR Data. The main bands of these products appear at the following wavenumbers cm^{-1}): (**1**) 1630 (vs), 1572 (m), 1485 (m), 1452 (s), 1388 (vs), 1224 (m), 1160 (w), 798 (w), 757 (s), 694 (s) 655 (s) 549 (w). (**2**) 1623 (vs), 1570 (m), 1447 (s), 1433 (s), 1393 (vs), 1220 (w), 1157 (w), 1051 (m), 1036 (m), 748 (s), 698 (s), 691 (s) 648 (s) 471 (m). (**3**) 1623 (vs), 1561 (m), 1447 (m), 1431 (m), 1396 (vs), 1220 (w), 1158 (w), 1042 (w), 1025 (w), 747 (s), 691 (s), 643 (m), 452 (m). (**4**) 1627 (vs), 1582 (vs), 1485 (w), 1445 (s), 1391 (vs), 1268 (w), 1228 (m), 1071 (w), 929 (m), 792 (s), 765 (s), 695 (s), 667 (s), 467 (w), 445 cm^{-1} (w). (**5**) 1619 (vs), 1566 (vs), 1448 (m), 1423 (s), 1388 (vs), 1267 (w), 1071 (w), 758 (s), 736 (s) 696 (m), 449. (**6**) 1621 (vs), 1560 (vs), 1416 (m), 1386 (vs), 1267 (w), 1067 (w), 756 (s), 716 (m), 710 (m), 449(w). The main differences in the two series (2-X and 3-X) are in the asymmetric stretching zone (ν_{as}) of the carboxylate: for 2-X there is only one band (~1620 cm^{-1}); however, for the 3-X this band is split into two bands (at ~1620 and 1570 cm^{-1}). The symmetric stretching zone (ν_s) always appears at ~1390 cm^{-1}. On the other hand, the substitution of Cl for Br does not change the spectrum appreciably; the fluoro derivative is different in both series.

Crystal Data Collection and Refinement. Crystals of **1** (0.57 × 0.19 × 0.19 mm), **5** (0.61 × 0.46 × 0.23 mm), and **6** (0.53 × 0.34 × 0.34 mm) were mounted on a Stoe AED2 four-circle diffractometer, using graphite-monochromated Kα radiation ($\lambda = 0.710\,73$ Å). Unit cell parameters were determined by least squares from the $\pm\omega$ values of 29 reflections for **1** ($14° < \theta < 18.5°$), 18 reflections for **5** ($14° < \theta < 17°$), and 16 reflections for **6** ($14° < \theta < 17.5°$). For **1**, 5111 independent reflections were measured in the range $2.54° < \theta < 25°$ at 223(2) K; for **5**, 7363 independent reflections were measured in the range $1.5° < \theta < 22.5°$ at 213(2) K; and for **6**, 10 299 independent reflections were measured in the range $1.8° < \theta < 25°$ at 213(2) K. The number of observed reflections [$I > 2\sigma(I)$] were 2778 for **1**, 3633 for **5**, and 3374 for **6**. In each case, two standard reflections were measured every hour and showed a small intensity variation (5% for **1**, 3% for **5**, and 1% for **6**). An empirical absorption correction was applied in the case of **6**[13] (DIFABS transmission factors minimum/maximum 0.187/1.00). Crystallographic data are shown in Table 1. The crystal structures were solved by direct methods and Fourier

(8) Gerbelen, N. V.; Timco, G. A.; Manole, O. S.; Struchkov, Y. T.; Batsanov, A. S.; Grebenzo, S. V. *Koord. Khim*. **1994**, *20*, 357.
(9) Zhang, S. W.; Wei, Y. G.; Liu, Q.; Shao, M. C. *Polyhedron* **1996,** *15*, 1041.
(10) Nakano, M.; Sorai, M.; Vincent, J. B.; Christou, G.; Jang, H. G.; Hendrickosn, D. N. *Inorg. Chem*. **1989,** *28*, 4608.
(11) Jang, H. G.; Vincent, J. B.; Nakano, M.; Huffman, J. C.; Christou, G.; Sorai, M.; Wittebort, R. J.; Hendrickson, D. N. *J. Am. Chem. Soc*. **1989**, *111*, 7778.
(12) Sala, T.; Sargent, M. V. *J. Chem. Soc., Chem. Commun*. **1978**, 253.
(13) Walker, N.; Stuart, D. DIFABS. *Acta Crystallogr*. **1983**, *A39*, 158.

Table 1. Crystallographic Data for **1 (2-F)**, **5 (3-Cl)**, and **6 (3-Br)**

	1	5	6
chem formula	$C_{57}H_{39}F_6Mn_3N_3O_{13}2(CH_3CN)$	$C_{52}H_{36}Cl_6Mn_3N_2O_{14}\cdot{}^1/_2(H_2O)$	$C_{52}H_{36}Br_6Mn_3N_2O_{14}\cdot{}^1/_4(H_2O)$
formula weight	1334.84	1299.36	1561.61
space group	*C*2/*c*	$P2_1/n$	$P2_1/n$
T (°C)	223(2)	213(2)	213(2)
a (Å)	15.774(2)	15.172(2)	15.553(3)
b (Å)	17.269(2)	17.603(2)	17.884(2)
c (Å)	21.411(2)	21.996(3)	21.997(4)
β	91.11(1)	106.300(10)	106.95(1)
V (Å$^{3)}$	5831.3(11)	5638.4(12)	5853(2)
Z	4	4	4
λ (Å)	0.710 73	0.710 73	0.710 73
ρ_{calcd} (g cm^{-3})	1.520	1.531	1.772
μ (mm^{-1})	0.708	0.987	4.773
*R*1[a]	0.0800	0.1175	0.1148
w*R*2[b]	0.2103	0.3362	0.2769

[a] $R1$ (obsd reflns) $= \sum||F_o| - |F_c||/\sum|F_o|$. [b] w$R2$ (obsd reflns) $= [\sum w(F_o^2 - F_c^2)^2/\sum wF_o^2]^{1/2}$.

syntheses using the program SHELXS[14] and refined by the full-matrix least-squares method using the program SHELXL-93.[15] The function minimized was $\sum w(|F_o|^2 - |F_c|^2)^2$, where $w = [(\sigma^2(I) + (k_1P)^2 + (k_2P)]^{-1}$ and $P = (|F_o|^2 + 2|F_c|^2)/3$: the values for k_1 were 0.1383 for **1**, 0.2591 for **5**, and 0.1624 for **6**. k_2 was 0.0 for all three structures. Complex neutral atom scattering factors were taken from *International Tables for X-ray Crystallography*. In **1**, the fluorobenzoate groups involving atoms F(1) and F(2) were disordered and two alternative positions were given for these atoms with occupancies of 0.5. A similar situation was observed in **5** with the benzoate groups involving atoms Cl(2) and Cl(6). Here the occupancies were found to be Cl(2/2B) 0.8/0.2 and Cl(6/6B) 0.7/0.3. In **6**, the benzoate groups involving atoms Br(2) and Br(6) were also disordered (occupancies 0.9/0.1 and 0.7/0.3). In both **5** and **6**, the pyridine rings involving atoms N(1) were fitted to those involving atom N(2) and refined as rigid groups. In most cases the hydrogen atoms were included in calculated positions as riding atoms ($U_{iso} = U_{eq}$(attached C atom) + 1.2). It was not possible to locate the H-atoms of the disordered molecules of solvent of crystallization. For **1**, 418 parameters were refined, 685 for **5**, and 683 for **6**. The maximun shift/esd and the mean shift/esd were −0.065 and 0.003 for **1**, 0.059 and 0.005 for **5**, and −0.140 and 0.005 for **6**. Maximum and minimum peaks in the final difference maps were 1.06 and −1.02 e Å^{-3} for **1**, 1.36 (near atom OW2) and −2.19 e Å^{-3} for **5**, and 1.50 and −1.76 e Å^{-3} for **6**. Figures 1−3 were drawn using the program PLATON.[16]

Spectral and Magnetic Measurements. IR spectra (4000−400 cm^{-1}) were recorded on KBr pellets with a Nicolet 520 FT-IR spectrometer. Magnetic measurements were carried out on polycrystalline samples (30−40 mg) with a pendulum-type magnetometer−susceptometer (MANICS DSM.8) equipped with an Oxford helium continuous-flow cryostat, working in the 4.2−300 K range, and a Drusch EAF 16UE electromagnet. The magnetic field was ∼1.2 T. The diamagnetic corrections were evaluated from Pascal's constants. To guarantee the accuracy of results especially in the low-temperature range, magnetic measurements were repeated with a Quantum Design MPMS SQUID susceptometer operating at a magnetic field of 0.5 T between 2 and 300 K. The fit was carried out by using the MINUIT minimization program of the CERN program libray (v. 92.1), CERN, Geneva, which ensures the accuracy of results so that the true minimum can be calculated. Magnetization measurements were carried out with the same Quantum Design MPMS SQUID susceptometer operating at 2.5 K between 0 and 50 000 G. EPR spectra were recorded on powder samples at X-band frequency with a Bruker 300E automatic spectrometer, varying the temperature from 4 to 77 K

Results and Discussion

Synthesis and Structures. Complex **1** represents the first example of a Mn_3O (III,III,II) with benzoato derivatives as bridging ligands and with three pyridines as terminal ligands. The only similar example reported so far was with acetate as the bridging ligand.[5] Complex **1** crystallizes in monoclinic space group *C*2/*c*. The data were collected at 223 K to avoid decomposition due to the loss of MeCN molecules. A PLATON projection is shown in Figure 1. Fractional coordinates and isotropic thermal parameters are listed in Table 2; selected bond lengths and angles are listed in Table 3. The overall complex has imposed C_2 symmetry so that Mn_3 is an isosceles triangle. The central O-atom O(12) lies on the C_2 axis and exactly in the plane of the Mn_3 triangle (0.000 Å). The O(12)−Mn distances are 1.871(3) Å for Mn(1) and Mn(1)# and 1.990(6) Å for Mn(2), respectively. The Mn−O(12)−Mn angles are all similar (Mn(1)−O(12)−Mn(1)# = 120.7 (3)°, Mn(1)#−O(12)−Mn(2) = 119.6(2)°, and Mn(1)−O(12)−Mn(2) = 119.6(2)°, respectively). The Mn(1) (and Mn(1)#) coordination geometry is slightly distorted octahedral, consisting of the oxygen of the central triangle, four oxygen atoms from bridging 2F-benzoato ligands, and a terminal pyridine nitrogen atom. The shortest distance is Mn(1)−O(12), 1.871(3) Å. Mn(2) also has distorted octahedral coordination, with the shortest distance corresponding also to Mn−O(12), 1.990(6) Å. In this case, the longest distance (2.234 Å) is to the nitrogen atom of the pyridine ligand *trans* to O(12). In fact, all bond distances to Mn(2) (average value 2.109 Å) are longer than those for Mn(1) and Mn(1)# (average value 2.048 Å), which can be interpreted as indicating that Mn-

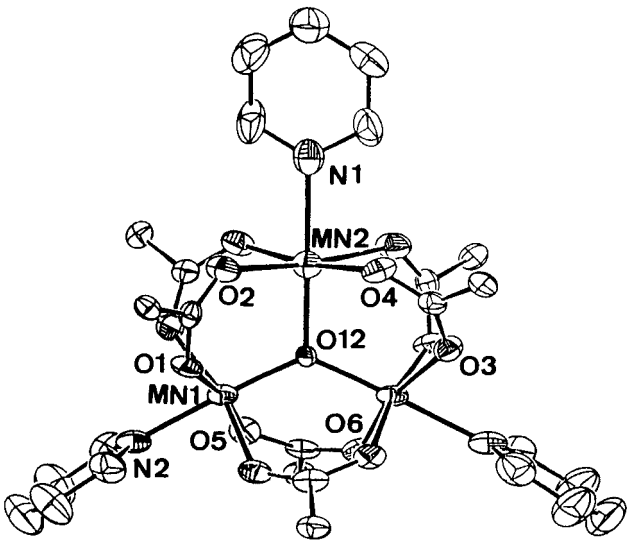

Figure 1. PLATON projection of $[Mn_3O(2F\text{-benzoato})_6(pyr)_3]2MeCN$ (**1**), which possess crystallographic C_2 symmetry. Thermal ellipsoids at the 50% probability level. The F-benzene moieties and the H-atoms have been omitted for clarity.

(14) Sheldrick, G. M. SHELXS. *Acta Crystallogr*. **1990**. *A46*, 467.
(15) Sheldrick, G. M. SHELXL. Program for crystal structure refinement. University of Göttingen, Göttingen, Germany, 1993.
(16) Spek, A. L. PLATON. *Acta Crystallogr*. **1993**, *A46*, C34.

Table 2. Atomic Coordinates ($\times 10^4$) and Equivalent Isotropic Displacement Parameters ($Å^2 \times 10^3$) for **1 (2-F)**

	x	*y*	*z*	*U*(eq)[a]
Mn(1)	872(1)	8473(1)	2918(1)	29(1)
Mn(2)	0	10161(1)	2500	30(1)
O(12)	0	9009(4)	2500	21(1)
O(1)	1811(3)	9022(3)	2467(2)	35(1)
O(2)	1359(3)	10243(3)	2361(3)	42(1)
O(3)	1018(3)	9247(3)	3680(2)	36(1)
O(4)	−201(3)	10253(3)	1558(2)	37(1)
O(5)	86(3)	7826(3)	3436(2)	34(1)
O(6)	998(3)	7593(3)	2219(2)	35(1)
N(1)	0	11455(6)	2500	44(2)
N(2)	1845(4)	7838(3)	3382(3)	36(2)
C(1)	505(6)	11842(6)	2893(4)	59(3)
C(2)	500(7)	12643(6)	2912(6)	80(4)
C(3)	0	13027(9)	2500	66(4)
C(4)	2503(5)	7613(5)	3089(5)	50(2)
C(5)	3119(7)	7149(7)	3380(5)	72(3)
C(6)	3025(7)	6900(6)	3960(6)	72(3)
C(7)	2290(7)	7142(6)	4272(5)	73(3)
C(8)	1729(6)	7615(6)	3967(4)	56(3)
F(1)	2766(5)	11085(4)	2689(4)	45(2)
F(1B)[b]	2910(7)	8799(6)	1511(5)	64(3)
C(9)	1886(4)	9743(4)	2326(3)	27(2)
C(10)	3122(5)	10647(4)	2261(4)	38(2)
C(11)	2761(4)	9944(4)	2088(3)	29(2)
C(12)	3921(5)	10854(5)	2062(5)	54(3)
C(13)	4333(5)	10369(5)	1661(5)	55(3)
C(14)	3970(6)	9672(5)	1486(4)	50(2)
C(15)	3210(5)	9463(5)	1694(4)	39(2)
C(16)	675(4)	9880(4)	3803(3)	27(2)
F(2)	1724(5)	9194(4)	4794(3)	32(2)
F(2B)[b]	−3(9)	11300(8)	4278(6)	87(4)
C(17)	843(4)	10214(4)	4438(3)	28(2)
C(18)	1377(5)	9853(5)	4881(4)	44(2)
C(19)	1504(6)	10165(6)	5478(4)	51(2)
C(20)	1121(6)	10855(5)	5633(4)	48(2)
C(21)	635(6)	11222(8)	5211(4)	48(2)
C(22)	493(5)	10906(5)	4613(4)	39(2)
C(23)	−638(5)	7547(4)	3295(3)	27(2)
F(3)	−2428(4)	7404(4)	3483(3)	84(2)
C(24)	−1048(5)	7092(4)	3811(4)	34(2)
C(25)	−1901(5)	7044(5)	3879(4)	47(2)
C(26)	−2271(7)	6677(7)	4376(5)	73(3)
C(27)	−1750(7)	6320(7)	4812(5)	73(3)
C(28)	−891(7)	6329(6)	4748(5)	69(3)
C(29)	−537(6)	6731(5)	4266(4)	45(2)
N(9)	3971(11)	8839(13)	4577(9)	208(10)
C(90)	3669(8)	9145(10)	4189(8)	108(5)
C(91)	3220(8)	9547(8)	3714(5)	86(4)

[a] *U*(eq) is defined as one-third of the trace of the orthogonalized U_{ij} tensor. [b] Occupancy 0.5.

(2) is in oxidation state +2, whereas Mn(1) and Mn(1)# are in oxidation state +3. This asymmetry is most noticeable in the Mn_3O central core with the long Mn(2)−O(12) distance leading to the Mn_3 triangle being isosceles rather than equilateral. The Mn(1)···Mn(1)# (3.253 Å) distance is significantly shorter than the Mn(1,1#)···Mn(2) distances (3.338 Å). In the acetato $Mn^{III,III,II}$ complex,[6] there is a crystallographic equivalence among the three manganese ions, but this was not found to be the case here; only two Mn atoms are equivalent.

Complex **5** crystallizes in monoclinic space group $P2_1/n$. The data were collected at 213 K. A PLATON projection is shown in Figure 2. Fractional coordinates and isotropic thermal parameters are listed in Table 4; selected bond lengths and angles are listed in Table 5. The complex again has distorted octahedral metal geometries and the overall "basic metal carboxylate" structure. The central O-atom O(13) lies almost in the plane of the Mn_3 triangle (0.017 Å). The O(13)−Mn distances are 1.831(9) Å for Mn(1), 1.835(9) Å for Mn(2) and 2.064(10) Å for Mn(3) (which has the H_2O molecule as terminal ligand). The Mn−O(13)−Mn angles are Mn(1)−O(13)−Mn(2) = 121.6 (5)°; Mn(1)−O(13)−Mn(3) = 119.3(5)° and Mn(2)−O(13)−Mn(3) = 119.0(5)°, respectively. The Mn coordination geometries are slightly distorted octahedra consisting of the oxygen of the central triangle, four oxygen atoms from bridging 2Cl-benzoato ligands, and a terminal oxygen (H_2O) or nitrogen (pyridine) atom. The *average* values for the five Mn−O bond distances are 2.017 Å for Mn(1), 2.014 Å for Mn(2), and 2.054 Å for Mn(3). This asymmetry is most noticeable in the Mn_3O central core with the long Mn(3)−O(13) distance, leading to the Mn_3 triangle being essentially isosceles rather than equilateral. The Mn(1)···Mn(2) distance (3.201 Å) is significantly shorter than the Mn(1,2)···Mn(3) distances (3.364 and 3.362 Å). For all these reasons, the Mn(3) atom can be assigned as the Mn^{II} center since all Mn(3) distances are longer than those for Mn(2) and Mn(1), as expected for the lower oxidation state. The same situation has been reported for the benzoate analog.[6] One of the pyridine rings is essentially coplanar with the Mn_3O plane while the other is almost perpendicular, probably due to steric interaction with the two 3-chlorobenzoate groups.

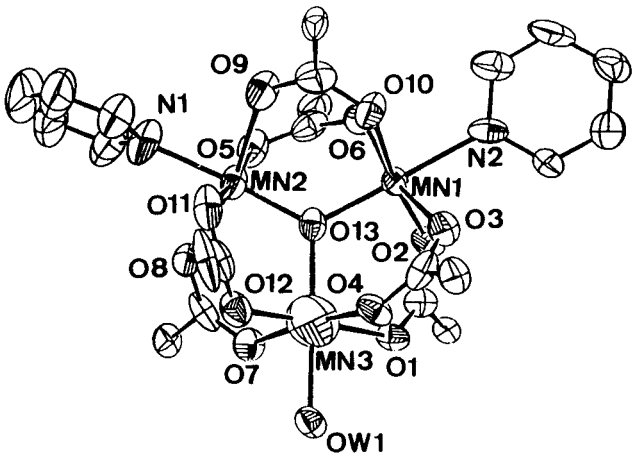

Figure 2. PLATON projection of $[Mn_3O(3Cl\text{-benzoato})_6(pyr)_2(H_2O)]\cdot {}^1/_2H_2O$ (**5**). Thermal ellipsoids at the 50% probability level. The Cl-benzene moieties and the H-atoms have been omitted for clarity.

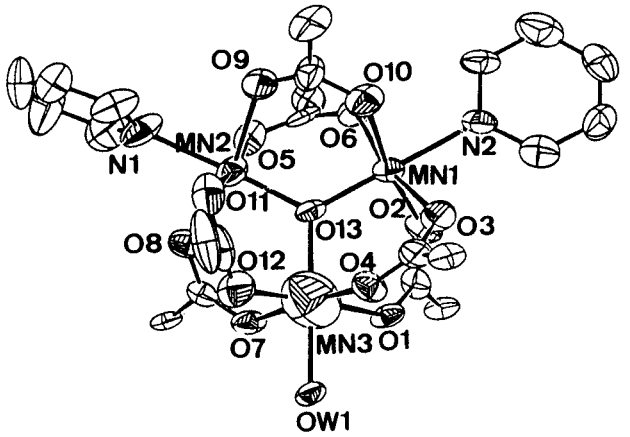

Figure 3. PLATON projection of $[Mn_3O(3Br\text{-benzoato})_6(pyr)_2(H_2O)]\cdot {}^1/_4H_2O$ (**6**). The Br-benzene moieties and the H-atoms have been omitted for clarity.

Complex **6** crystallizes in monoclinic space group $P2_1/n$ and is, in fact, isostructural with complex **5.** The data were collected at 213 K. A PLATON projection is shown in Figure 3. Fractional coordinates and isotropic thermal parameters are listed in Table 6; selected bond lengths and angles are listed in Table 7. The central O-atom O(13) is slightly displaced from the plane of the Mn_3 triangle (0.038 Å). The O(13)−Mn distances are

Table 3. Selected Bond Lengths (Å) and Angles (deg) for **1 (2-F)**

Mn(1)−O(12)	1.871(3)	Mn(2)−O(4)#1	2.042(5)
Mn(1)−O(5)	2.017(5)	Mn(2)−O(2)	2.174(5)
Mn(1)−O(1)	2.021(5)	Mn(2)−O(2)#1	2.174(5)
Mn(1)−N(2)	2.118(7)	Mn(2)−N(1)	2.234(10)
Mn(1)−O(3)	2.118(5)	O(12)−Mn(1)#1	1.871(3)
Mn(1)−O(6)	2.145(5)	Mn(1)−Mn(2)	3.338(5)
Mn(2)−O(12)	1.990(6)	Mn(1)−Mn(1)#1	3.253(3)
Mn(2)−O(4)	2.041(5)		
O(12)−Mn(1)−O(5)	94.8(2)	O(4)−Mn(2)−O(4)#1[a]	171.1(3)
O(12)−Mn(1)−O(1)	94.5(2)	O(12)−Mn(2)−O(2)	93.74(14)
O(5)−Mn(1)−O(1)	170.7(2)	O(4)−Mn(2)−O(2)	89.6(2)
O(12)−Mn(1)−N(2)	178.4(2)	O(4)#1−Mn(2)−O(2)	89.8(2)
O(5)−Mn(1)−N(2)	84.4(2)	O(12)−Mn(2)−O(2)#1	93.74(14)
O(1)−Mn(1)−N(2)	86.3(2)	O(4)−Mn(2)−O(2)#1	89.8(2)
O(12)−Mn(1)−O(3)	97.2(2)	O(4)#1−Mn(2)−O(2)#1	89.6(2)
O(5)−Mn(1)−O(3)	89.2(2)	O(2)−Mn(2)−O(2)#1	172.5(3)
O(1)−Mn(1)−O(3)	90.1(2)	O(12)−Mn(2)−N(1)	180.00(3)
N(2)−Mn(1)−O(3)	84.2(2)	O(4)−Mn(2)−N(1)	85.54(14)
O(12)−Mn(1)−O(6)	95.4(2)	O(4)#1−Mn(2)−N(1)	85.54(14)
O(1)−Mn(1)−O(6)	85.4(2)	O(2)#1−Mn(2)−N(1)	86.26(14)
N(2)−Mn(1)−O(6)	83.4(2)	Mn(1)#1−O(12)−Mn(1)	120.7(3)
O(3)−Mn(1)−O(6)	167.0(2)	Mn(1)#1−O(12)−Mn(2)	119.6(2)
O(12)−Mn(2)−O(4)	94.46(14)	Mn(1)−O(12)−Mn(2)	119.6(2)
O(12)−Mn(2)−O(4)#1	94.46(14)		

[a] Symmetry transformation used to generate equivalent atoms: (#1) $-x, y, -z + {}^1/_2$.

Table 4. Atomic Coordinates ($\times 10^4$) and Equivalent Isotropic Displacement Parameters ($Å^2 \times 10^3$) for **5 (3-Cl)**[a]

	x	*y*	*z*	*U*(eq)[b]		*x*	*y*	*z*	*U*(eq)
Mn(1)	471(1)	8422(1)	2221(1)	32(1)	O(6)	1100(7)	9137(6)	3028(5)	49(3)
Mn(2)	−872(2)	9820(1)	2234(1)	41(1)	C(25)	1019(12)	9834(9)	3060(7)	44(4)
Mn(3)	−612(3)	9252(2)	835(2)	116(2)	C(26)	1851(11)	10260(9)	3441(7)	45(4)
O(13)	−314(6)	9165(5)	1808(4)	37(2)	C(27)	2698(13)	9958(9)	3573(9)	64(5)
OW	−924(7)	9369(5)	−163(4)	42(2)	C(28)	3438(15)	10360(12)	3865(12)	96(7)
N(1)	−1596(8)	10559(6)	2623(6)	66(4)	C(29)	3366(15)	11064(13)	4078(11)	100(8)
C(1)	−2411(8)	10374(6)	2704(6)	90(7)	C(30)	2548(15)	11407(10)	3978(8)	65(5)
C(2)	−2969(7)	10865(9)	2910(7)	105(8)	C(31)	1800(12)	10997(10)	3679(8)	58(5)
C(3)	−2672(11)	11610(8)	3065(8)	104(8)	Cl(4)	970(7)	13403(4)	2239(3)	154(4)
C(4)	−1843(12)	11793(5)	2992(8)	120(10)	O(7)	−345(7)	10416(6)	840(5)	48(3)
C(5)	−1317(9)	11289(7)	2775(7)	100(8)	O(8)	−823(7)	10779(5)	1662(5)	43(3)
N(2)	1403(8)	7610(7)	2710(5)	38(3)	C(32)	−492(9)	10890(8)	1224(9)	43(4)
C(6)	1582(12)	7495(9)	3336(7)	54(4)	C(33)	−220(10)	11716(8)	1123(7)	43(4)
C(7)	2225(14)	6999(10)	3679(8)	71(6)	C(34)	85(13)	12164(9)	1628(9)	64(5)
C(8)	2728(14)	6559(9)	3365(9)	63(5)	C(35)	434(14)	12883(11)	1577(10)	75(6)
C(9)	2540(13)	6666(10)	2733(9)	62(5)	C(36)	439(15)	13134(10)	990(11)	86(7)
C(10)	1900(11)	7178(8)	2411(7)	44(4)	C(37)	69(12)	12695(8)	476(10)	61(5)
Cl(1)	471(4)	5453(3)	2756(3)	91(2)	C(38)	−242(11)	11990(8)	515(8)	50(4)
O(1)	743(6)	9075(5)	860(4)	38(2)	Cl(5)	−1232(3)	5759(2)	3976(2)	66(1)
O(2)	1469(6)	8773(5)	1863(4)	39(2)	O(9)	−1007(8)	9056(6)	2939(5)	57(3)
C(11)	1449(10)	9042(8)	1312(7)	38(4)	O(10)	−374(7)	8009(5)	2676(5)	47(3)
C(12)	2682(8)	4339(7)	3775(6)	25(3)	C(39)	−867(12)	8351(10)	2966(8)	52(4)
C(13)	2535(10)	4333(8)	4347(7)	40(4)	C(40)	−1364(7)	7879(5)	3331(5)	44(4)
C(14)	1740(13)	4675(12)	4447(9)	70(5)	C(41)	−2054(8)	8196(5)	3553(7)	79(6)
C(15)	1103(11)	4990(10)	3984(9)	55(4)	C(42)	−2489(8)	7760(7)	3910(7)	103(9)
C(16)	1276(11)	5017(9)	3379(9)	60(5)	C(43)	−2234(8)	7006(6)	4045(6)	73(6)
C(17)	2065(10)	4658(8)	3278(8)	48(4)	C(44)	−1544(8)	6690(4)	3823(6)	57(5)
Cl(2)	−952(6)	4611(3)	1166(5)	127(4)	C(45)	−1109(6)	7126(5)	3466(5)	50(4)
Cl(2B)	−3178(31)	6059(19)	−442(17)	151(18)	Cl(6)	−5238(7)	8056(7)	1541(6)	141(4)
O(3)	2(7)	7543(5)	1547(5)	42(2)	Cl(6B)	−4492(12)	7434(15)	−307(7)	116(9)
O(4)	−937(7)	8138(5)	706(5)	48(3)	O(11)	−2129(7)	9443(6)	1730(7)	56(3)
C(18)	−629(11)	7545(9)	1045(8)	46(4)	O(12)	−1958(7)	9433(6)	771(6)	56(3)
C(19)	−1105(11)	6796(8)	792(8)	44(4)	C(46)	−2354(11)	9271(9)	1157(11)	51(4)
C(20)	−830(13)	6155(9)	1066(10)	72(6)	C(47)	−3277(7)	8852(7)	941(8)	83(7)
C(21)	−1279(16)	5473(12)	807(13)	91(7)	C(48)	−3839(10)	8755(8)	1337(7)	91(8)
C(22)	−1975(18)	5456(13)	308(14)	105(8)	C(49)	−4636(9)	8325(9)	1136(10)	104(10)
C(23)	−2297(15)	6150(13)	−7(12)	98(8)	C(50)	−4873(8)	7993(9)	539(11)	137(13)
C(24)	−1830(12)	6818(9)	274(9)	66(5)	C(51)	−4311(12)	8090(10)	142(9)	203(21)
Cl(3)	2446(4)	2301(3)	4241(3)	101(2)	C(52)	−3513(10)	8520(10)	343(8)	132(12)
O(5)	288(7)	10219(5)	2803(5)	47(3)	OW2	−691(26)	9501(20)	5089(22)	175(22)

[a] Pyridine ring N1−C5 has been fitted to pyridine ring N2−C10 as a rigid group. Occupancy Cl2 0.8, Cl2B 0.2, Cl6 0.7, Cl6B 0.3, OW2 0.5. [b] *U*(eq) is defined as one-third of the trace of the orthogonalized U_{ij} tensor.

1.824(10) Å for Mn(1), 1.830(10) Å for Mn(2), and 2.066(12) Å for Mn(3) (which also has the H_2O molecule as terminal ligand). The Mn−O(13)−Mn angles are Mn(1)−O(13)−Mn(2) = 122.4(5)°; Mn(1)−O(13)−Mn(3) = 119.5(5)°, and Mn-

Table 5. Main Bond Lengths (Å) and Angles (deg) for **5 (3-Cl)**[a]

Mn(1)−O(13)	1.831(9)	Mn(2)−N(1)	2.038(9)
Mn(1)−O(10)	1.973(10)	Mn(2)−O(9)	2.105(11)
Mn(1)−O(2)	1.992(10)	Mn(2)−O(8)	2.119(10)
Mn(1)−N(2)	2.084(12)	Mn(2)−Mn(3)	3.362(5)
Mn(1)−O(3)	2.123(10)	Mn(3)−O(4)	2.023(10)
Mn(1)−O(6)	2.166(10)	Mn(3)−O(12)	2.031(12)
Mn(1)−Mn(2)	3.201(3)	Mn(3)−O(1)	2.065(10)
Mn(1)−Mn(3)	3.364(5)	Mn(3)−O(13)	2.064(10)
Mn(2)−O(13)	1.835(9)	Mn(3)−O(7)	2.088(11)
Mn(2)−O(5)	1.979(11)	Mn(3)−OW1	2.123(10)
Mn(2)−O(11)	2.031(12)		
O(13)−Mn(1)−O(10)	95.2(4)	N(1)−Mn(2)−O(9)	85.6(4)
O(13)−Mn(1)−O(2)	92.5(4)	O(13)−Mn(2)−O(8)	95.7(4)
O(10)−Mn(1)−O(2)	171.7(4)	O(5)−Mn(2)−O(8)	85.4(4)
O(13)−Mn(1)−N(2)	177.6(4)	O(11)−Mn(2)−O(8)	96.9(4)
O(10)−Mn(1)−N(2)	86.0(4)	N(1)−Mn(2)−O(8)	81.6(4)
O(2)−Mn(1)−N(2)	86.3(4)	O(9)−Mn(2)−O(8)	166.7(4)
O(13)−Mn(1)−O(3)	97.5(4)	O(4)−Mn(3)−O(12)	86.7(5)
O(10)−Mn(1)−O(3)	87.0(4)	O(4)−Mn(3)−O(1)	93.4(4)
O(2)−Mn(1)−O(3)	95.4(4)	O(12)−Mn(3)−O(1)	177.6(5)
N(2)−Mn(1)−O(3)	84.7(4)	O(4)−Mn(3)−O(13)	92.8(4)
O(13)−Mn(1)−O(6)	93.8(4)	O(12)−Mn(3)−O(13)	90.4(5)
O(10)−Mn(1)−O(6)	89.9(4)	O(1)−Mn(3)−O(13)	92.0(4)
O(2)−Mn(1)−O(6)	86.2(4)	O(4)−Mn(3)−O(7)	172.5(5)
N(2)−Mn(1)−O(6)	84.1(4)	O(12)−Mn(3)−O(7)	92.1(5)
O(3)−Mn(1)−O(6)	168.5(4)	O(1)−Mn(3)−O(7)	87.6(4)
O(13)−Mn(2)−O(5)	95.1(4)	O(13)−Mn(3)−O(7)	94.7(4)
O(13)−Mn(2)−O(11)	90.7(4)	O(4)−Mn(3)−OW1	88.5(4)
O(5)−Mn(2)−O(11)	173.5(5)	O(12)−Mn(3)−OW1	89.2(5)
O(13)−Mn(2)−N(1)	174.1(5)	O(1)−Mn(3)−OW1	88.5(4)
O(5)−Mn(2)−N(1)	89.9(5)	O(13)−Mn(3)−OW1	178.6(4)
O(11)−Mn(2)−N(1)	84.5(5)	O(7)−Mn(3)−OW1	84.0(4)
O(13)−Mn(2)−O(9)	97.4(4)	Mn(1)−O(13)−Mn(2)	121.6(5)
O(5)−Mn(2)−O(9)	90.8(4)	Mn(1)−O(13)−Mn(3)	119.3(5)
O(11)−Mn(2)−O(9)	85.6(5)	Mn(2)−O(13)−Mn(3)	119.0(5)

[a] Symmetry transformations used to generate equivalent atoms: (#1) $-x + 1/2, y + 1/2, -z + 1/2$; (#2) $-x + 1/2, y - 1/2, -z + 1/2$; (#3) $x, y - 1, z$; (#4) $x, y + 1, z$.

(2)−O(13)−Mn(3) = 118.0(5)°, respectively. The Mn coordination geometries are slightly distorted octahedra with the oxygen of the central triangle, four oxygen atoms from bridging 2Br-benzoato ligands, and a terminal oxygen (H_2O) or nitrogen (pyridine) atom completing the coordination. The *average* values for the five Mn−O bond distances are 2.033 Å for Mn(1), 2.021 Å for Mn(2), and 2.042 Å for Mn(3). This asymmetry is most noticeable in the Mn_3O central core with the long Mn(3)−O(13) distance leading to the Mn_3 triangle being essentialy isosceles rather than equilateral. The Mn(1)···Mn(2) distance 3.202 Å is significantly shorter than the Mn(1,2)···Mn(3) distances (3.362 and 3.340 Å). For all these reasons, as in the 3-cloro derivative, the Mn(3) atom can be assigned as the Mn^{II} center since all Mn(3)−O distances are longer than those for Mn(2) and Mn(1), as expected for the lower oxidation state. As in the 2-Cl derivative, one of the pyridine rings is essentially coplanar with the Mn_3O plane while the other is almost perpendicular.

Susceptibility and Magnetization Studies. Variable temperature (2−300 K) magnetic susceptibility data were collected for microcrystalline samples of compounds **1**−**6**. In all six cases, the magnetic measurements were taken at least twice from different samples and with a different magnetometer (see Experimental Section). The spin Hamiltonian that describes the isotropic magnetic exchange interaction in a triangulated trinuclear complex is given in equation 2. If it is assumed that

$$H = -2[J_{12}(S_1S_2) + J_{23}(S_2S_3) + J_{31}(S_3S_1)] \qquad (2)$$

the two Mn^{III} ions are equivalent, then there are two exchange parameters, $J = J_{12} = J_{31}$ for the Mn^{II}−Mn^{III} interactions and $J^* = J_{23}$ for the Mn^{III}−Mn^{III} interaction. Using this model,

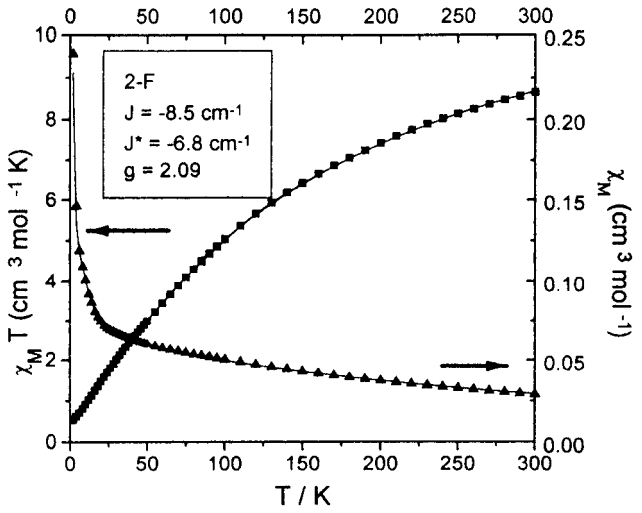

Figure 4. Plot of χ_M and $\chi_M T$ vs temperature for $[Mn_3O(2F\text{-benzoato})_6(pyr)_3]MeCN$ (**1**) as a representative example of the six complexes. Data were collected in an applied field of 5.00 kG. The solid lines result from a fit of the data to the appropriate theoretical equation; see Table 8 for magnetic parameters for all six complexes.

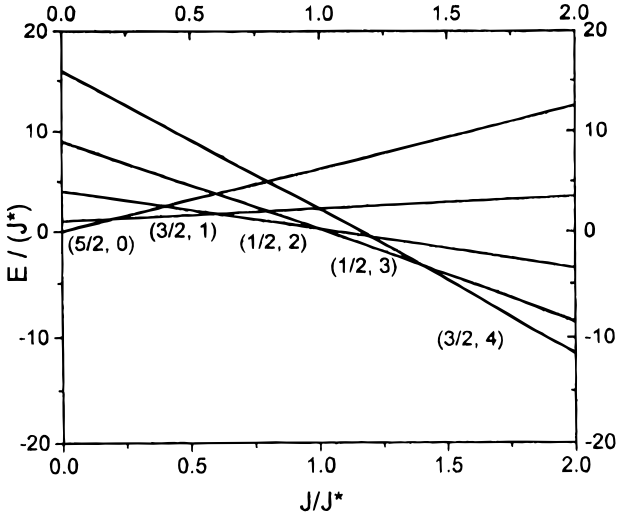

Figure 5. Eigenvalues of $H = -J(S_T^2 - S_A^2) - J^*S_A^2$ for $J < 0$ and $J^* < 0$ in units of J^*. States are labeled as (S_T, S_A), where S_T is the total spin and S_A is the value resulting from coupling the spins of the two Mn^{III} ions. Only the ground states are plotted. For a more general plot, see ref 2.

Vincent *et al*. derived the formula for the molar susceptibility vs $x = J/kT$ and $y = J^*/kT$ in a previous study.[6] Applying this Hamiltonian and the mathematical expression given by Vincent *et al*.,[6] the best-fit *J*, *J**, and *g* parameters are given in Table 8. As a representative example, the experimental and theoretical curves of χ_M and $\chi_M T$ vs *T* for **1** are shown in Figure 4. In order to understand the relation between *J*/*J** and the ground state, the linear variation of the ground states is plotted for several *J*/*J** ratios in Figure 5. This is only a part of the complete plot previously reported by McCusker *et al*.[2] As can be clearly seen from the *J*/*J** ratio, the ground state for complexes **2** and **3** is $3/2$, for complexes **2**, **4**, and **5** the ground state is undoubtedly $1/2$, and for **6** the ground state is either $1/2$ or $3/2$. This was confirmed by magnetization measurements vs H at 2 K. The results are plotted in Figure 6. The results coincided with the susceptibility measurements: for 2-Cl and 2-Br the $M/N\beta$ values tend to ∼2.3, which is inconsistent with a $S = 1/2$ ground state but is consistent for a $3/2$ ground state, as indicated by McCusker *et al*. for the acetate analogue.[2] For 2-F, 3-Cl, and 3-F the value of $M/N\beta$ tends to 1.2, consistent

Table 6. Atomic Coordinates ($\times 10^4$) and Equivalent Isotropic Displacement Parameters ($Å^2 \times 10^3$) for **6 (3-Br)**

	x	*y*	*z*	*U*(eq)[a]		*x*	*y*	*z*	*U*(eq)
Mn(1)	496(2)	8415(1)	2208(1)	37(1)	O(6)	1124(8)	9117(6)	3007(5)	48(3)
Mn(2)	−818(2)	9787(1)	2228(1)	46(1)	C(25)	1018(13)	9807(10)	3065(8)	43(4)
Mn(3)	−588(4)	9251(3)	829(3)	160(2)	C(26)	1878(12	10234(9)	3459(9)	46(4)
O(13)	−265(7)	9155(5)	1806(5)	34(3)	C(27)	2670(15)	9915(11)	3548(9)	66(6)
OW1	−912(7)	9376(6)	−180(5)	40(3)	C(28)	3440(18)	10278(13)	3843(13)	99(9)
N(1)	−1543(9)	10512(6)	2643(6)	64(5)	C(29)	3358(16)	11013(14)	4109(11)	90(8)
C(1)	−2369(10)	10285(7)	2703(7)	91(8)	C(30)	2543(15)	11318(10)	4009(9)	61(6)
C(2)	−2880(10)	10776(11)	2946(9)	115(10)	C(31)	1777(12)	10918(11)	3678(9)	58(5)
C(3)	−2565(13)	11493(9)	3128(8)	113(10)	Br(4)	1082(2)	13388(1)	2280(1)	116(1)
C(4)	−1739(14)	11720(6)	3068(9)	123(11)	O(7)	−339(8)	10383(5)	845(5)	48(3)
C(5)	1228(10)	11230(7)	2825(8)	107(9)	O(8)	−750(8)	10749(5)	1676(5)	46(3)
N(2)	1415(9)	7617(7)	2682(7)	42(3)	C(32)	−458(10)	10881(8)	1217(8)	35(4)
C(6)	1610(12)	7530(9)	3313(8)	48(5)	C(33)	−226(11)	11664(9)	1117(8)	38(4)
C(7)	2222(16)	7027(11)	3645(10)	75(7)	C(34)	132(11)	12109(10)	1629(8)	47(5)
C(8)	2657(13)	6581(10)	3308(11)	59(6)	C(35)	478(13)	12820(10)	1553(10)	59(5)
C(9)	2486(15)	6680(11)	2688(10)	70(6)	C(36)	416(14)	13100(10)	963(12)	73(7)
C(10)	1846(13)	7182(10)	2383(9)	56(5)	C(37)	4(13)	12653(9)	430(9)	55(5)
Br(1)	484(2)	5493(1)	2725(1)	86(1)	C(38)	−251(12)	11933(9)	519(9)	58(6)
O(1)	735(7)	9093(6)	852(5)	40(3)	Br(5)	−1210(2)	5676(1)	3931(1)	73(1)
O(2)	1467(7)	8757(6)	1842(6)	50(3)	O(9)	−958(9)	9003(6)	2925(6)	64(4)
C(11)	1444(11)	9047(9)	1306(9)	42(4)	O(10)	−324(9)	7987(6)	2678(6)	58(3)
C(12)	2719(11)	4331(8)	3770(8)	37(4)	C(39)	−849(13)	8329(10)	2929(9)	56(5)
C(13)	2577(11)	4288(11)	4355(10)	55(5)	C(40)	−1340(10)	7829(6)	3261(7)	62(6)
C(14)	1850(17)	4595(13)	4474(10)	78(7)	C(41)	−2065(11)	8128(5)	3426(9)	133(13)
C(15)	1200(15)	4965(12)	4017(10)	69(6)	C(42)	−2531(10)	7691(8)	3748(9)	120(11)
C(16)	1344(13)	4986(10)	3399(11)	69(7)	C(43)	−2270(10)	6955(7)	3903(8)	94(8)
C(17)	2078(12)	4680(8)	3273(9)	46(5)	C(44)	−1545(9)	6657(5)	3737(7)	64(6)
Br(2)	−947(2)	4585(1)	1093(2)	128(2)	C(45)	−1079(8)	7094(6)	3416(6)	54(5)
Br(2B)	−3479(15)	6123(12)	−339(11)	75(7)	Br(6)	−5173(3)	8079(2)	1540(3)	125(2)
O(3)	−6(8)	7545(6)	1500(6)	49(3)	Br(6B)	−4584(7)	7510(8)	−319(5)	139(5)
O(4)	−923(8)	8153(5)	711(5)	50(3)	O(11)	−2026(9)	9411(6)	1725(8)	64(4)
C(18)	−649(12)	7567(10)	1006(9)	49(5)	O(12)	−1872(9)	9438(9)	766(7)	69(4)
C(19)	−1103(12)	6847(8)	770(8)	43(4)	C(46)	−2245(14)	9284(10)	1114(14)	67(7)
C(20)	−833(14)	6172(10)	1025(9)	68(6)	C(47)	−3193(8)	8845(6)	945(10)	104(10)
C(21)	−1319(15)	5530(11)	747(12)	74(6)	C(48)	−3730(13)	8719(6)	1341(8)	113(11)
C(22)	−2054(15)	5561(12)	250(12)	93(8)	C(49)	−4537(12)	8334(6)	1114(11)	133(15)
C(23)	−2349(17)	6246(12)	−12(14)	112(10)	C(50)	−4807(7)	8076(7)	491(11)	194(26)
C(24)	−1867(14)	6890(11)	241(11)	75(6)	C(51)	−4270(11)	8202(7)	95(8)	204(24)
Br(3)	2456(2)	2292(1)	4292(2)	108(1)	C(52)	−3463(10)	8587(6)	322(9)	150(16)
O(5)	337(8)	10184(6)	2817(6)	51(3)	OW2	−3959(26)	4258(7)	144(18)	59(16)

[a] *U*(eq) is defined as one-third of the trace of the orthogonalized U_{ij} tensor.

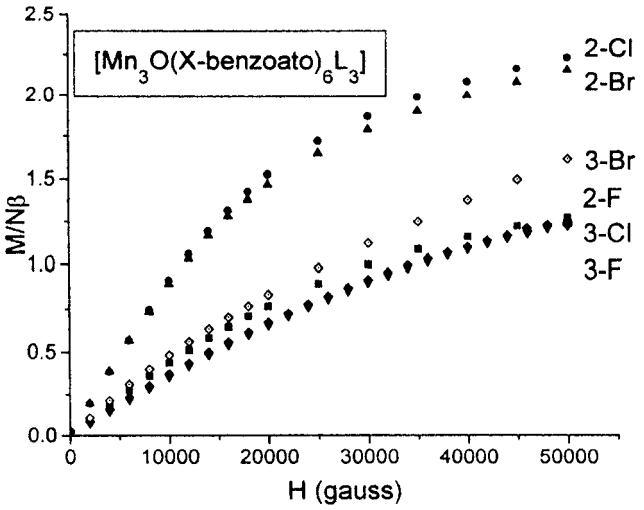

Figure 6. Magnetization plots ($M/N\beta$) vs H (G) for the six new complexes. The specific complex is indicated for each plot.

with a $^1/_2$ ground state, and for 3-Br, $M/N\beta$ value tends to 1.6, greater for a pure $^1/_2$ ground state but lower for a pure $^3/_2$ ground state: as in the susceptibility measurements a mixed ground state was observed. Effectively, a J/J^* ratio of 1.38 almost represents the crossing point for the $^1/_2$ and $^3/_2$ ground states (Figure 5). As reported by McCusker *et al.*[2] for the acetato trinuclear analogue, when the ground state is $^3/_2$ the value of $M/N\beta$ is not 3 (as expected for three electrons) but substantially lower (~2.3). This is because the zero-field splitting (D parameter) gives a net stabilization of the $m_s \pm {}^1/_2$ component of the $S = {}^3/_2$ ground state, which reduces the moment from the expected value based solely upon an unsplit $S = {}^3/_2$ state. This is not surprising since both of the high-spin Mn^{III} ions are expected to contribute substantial zero-field effects due to the Jahn−Teller distortion in Mn^{III} complexes. EPR experiments were carried out in all cases to distinguish between these two possible ground states, $^3/_2$ or $^1/_2$, and to corroborate the magnetic findings.

Electron Paramagnetic Resonance Spectroscopy. EPR spectroscopy is very useful in studying polynuclear manganese complexes with half-integer spin states. McCusker *et al.* previously reported a very complete treatment of the epr spectra for these kinds of trinuclear complex with $^3/_2$ or $^1/_2$ ground state.[2] In general, for complexes with a $S = {}^3/_2$ ground state, there is a strong signal in the $g \approx 4$ region and a weak signal in the $g \approx 2$ region. The intensity of the $g \approx 4$ signal decreases with temperature, indicating a depopulation of this state as the temperature is increased. In contrast, the small band at $g \approx 2$ increases when the temperature increases; at 77 K only this band appears. Complexes whose ground state is $^1/_2$ only show a broad signal centered at $g \approx 2$ which becomes sharper when the temperature increases. The X-band epr spectra for a polycrystalline sample of complex **3** in the range 4−250 K are shown in Figure 7. These spectra clearly show that the ground state

Table 7. Selected Bond Lengths (Å) and Angles (deg) for **6 (3-Br)**[a]

Mn(1)−O(13)	1.824(10)	Mn(2)−N(1)	2.095(10)
Mn(1)−O(2)	2.003(12)	Mn(2)−O(8)	2.127(11)
Mn(1)−O(10)	2.012(12)	Mn(2)−O(9)	2.134(11)
Mn(1)−N(2)	2.072(13)	Mn(2)−Mn(3)	3.340(7)
Mn(1)−O(6)	2.149(11)	Mn(3)−O(12)	1.99(2)
Mn(1)−O(3)	2.179(11)	Mn(3)−O(4)	2.028(11)
Mn(1)−Mn(2)	3.202(3)	Mn(3)−O(7)	2.060(11)
Mn(1)−Mn(3)	3.362(7)	Mn(3)−O(1)	2.064(12)
Mn(2)−O(13)	1.830(10)	Mn(3)−O(13)	2.066(12)
Mn(2)−O(11)	2.00(2)	Mn(3)−OW1	2.140(12)
Mn(2)−O(5)	2.015(12)		
O(13)−Mn(1)−O(2)	92.3(4)	N(1)−Mn(2)−O(8)	82.5(5)
O(13)−Mn(1)−O(10)	96.1(5)	O(13)−Mn(2)−O(9)	97.0(5)
O(2)−Mn(1)−O(10)	171.1(5)	O(11)−Mn(2)−O(9)	84.3(6)
O(13)−Mn(1)−N(2)	176.9(5)	O(5)−Mn(2)−O(9)	91.6(5)
O(2)−Mn(1)−N(2)	85.6(5)	N(1)−Mn(2)−O(9)	85.0(5)
O(10)−Mn(1)−N(2)	85.9(5)	O(8)−Mn(2)−O(9)	166.8(5)
O(13)−Mn(1)−O(6)	92.8(4)	O(12)−Mn(3)−O(4)	86.5(6)
O(2)−Mn(1)−O(6)	86.2(5)	O(12)−Mn(3)−O(7)	90.9(6)
O(10)−Mn(1)−O(6)	90.4(5)	O(4)−Mn(3)−O(7)	173.5(6)
N(2)−Mn(1)−O(6)	84.8(5)	O(12)−Mn(3)−O(1)	176.9(7)
O(13)−Mn(1)−O(3)	97.1(4)	O(4)−Mn(3)−O(1)	95.0(5)
O(2)−Mn(1)−O(3)	94.9(4)	O(7)−Mn(3)−O(1)	87.3(5)
O(10)−Mn(1)−O(3)	87.0(5)	O(12)−Mn(3)−O(13)	91.3(6)
N(2)−Mn(1)−O(3)	85.4(5)	O(4)−Mn(3)−O(13)	91.6(5)
O(6)−Mn(1)−O(3)	170.0(4)	O(7)−Mn(3)−O(13)	94.4(5)
O(13)−Mn(2)−O(11)	91.0(5)	O(1)−Mn(3)−O(13)	91.4(5)
O(13)−Mn(2)−O(5)	94.7(5)	O(12)−Mn(3)−OW1	89.0(6)
O(11)−Mn(2)−O(5)	173.4(6)	O(4)−Mn(3)−OW1	89.7(5)
O(13)−Mn(2)−N(1)	175.2(5)	O(7)−Mn(3)−OW1	84.3(5)
O(11)−Mn(2)−N(1)	84.9(6)	O(1)−Mn(3)−OW1	88.3(5)
O(5)−Mn(2)−N(1)	89.6(5)	O(13)−Mn(3)−OW1	178.7(5)
O(13)−Mn(2)−O(8)	95.8(4)	Mn(1)−O(13)−Mn(2)	122.4(5)
O(11)−Mn(2)−O(8)	98.7(5)	Mn(1)−O(13)−Mn(3)	119.5(5)
O(5)−Mn(2)−O(8)	84.1(5)	Mn(2)−O(13)−Mn(3)	118.0(5)

[a] Symmetry transformations used to generate equivalent atoms: (#1) $-x + {}^1/_2, y + {}^1/_2, -z + {}^1/_2$; (#2) $-x + {}^1/_2, y - {}^1/_2, -z + {}^1/_2$; (#3) $x, y - 1, z$; (#4) $x, y + 1, z$.

Table 8. Best-Fitted J, J^*, and g Parameters for **1**−**6** from the Hamiltonian Given in the Text and the Mathematical Expression given in Ref 5

compound	J (cm^{-1})	J^* (cm^{-1})	g	J/J^*	ground state[a]
2-F (**1**)	−8.5	−6.8	2.09	1.25	$^1/_2$
2-Cl (**2**)	−4.8	−2.9	2.08	1.65	$^3/_2$
2-Br (**3**)	−3.9	−2.4	2.05	1.625	$^3/_2$
3-F (**4**)	−7.05	−5.9	2.10	1.19	$^1/_2$
3-Cl (**5**)	−6.8	−5.5	2.10	1.13	$^1/_2$
3-Br (**6**)	−4.7	−3.4	2.05	1.38	$^1/_2$, $^3/_2$

[a] The ground state is taken from Figure 5 (see text).

of the complex **3** has an $S = {}^3/_2$, in agreement with the fit of susceptibility and magnetization measurements. This conclusion is based on the finding that at 4 K there is a strong, highly asymmetric signal in the $g \approx 4$ region. The intensity of this signal decreases with increasing temperature, indicating a depopulation of this state as the temperature is increased. This temperature dependence is consistent with the lowest energy state, that is the $m_s = \pm{}^1/_2$ Kramers doublet from the $S = {}^3/_2$ state. For **2**, the pattern is very similar. In contrast, for complexes with a $S = {}^1/_2$ ground state (according to susceptibility and magnetization measurements) (2-F, 3-Cl, 3-F), the epr spectra are very similar to those reported by McCusker *et al.* for the benzoato analogue,[2] whose ground state is also $^1/_2$. In Figure 8, the epr spectra for a polycrystalline sample of **1** in the range 4−290 K are shown. Bands are always centered at $g \approx 2$. These spectra clearly show that there is a change in the ground state relative to complexes **2** and **3**. The epr spectrum run at 4 K should, thus, be dominated by a signal from the $m_s = \pm{}^1/_2$ ($S = {}^1/_2$) Kramers doublet ground state. There could be a very small contribution from the low-lying $S = {}^3/_2$ excited

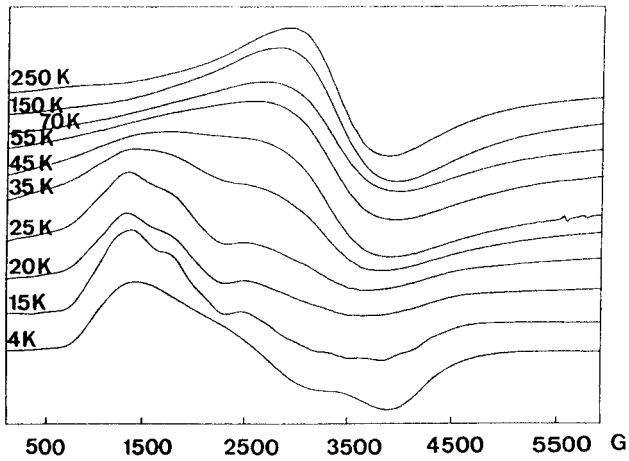

Figure 7. Temperature dependence of the X-band epr spectra of a powdered sample of $[Mn_3O(2Br\text{-benzoato})_6(pyr)_3]$ (**3**) (spin ground state $^3/_2$).

state. This is, in fact, what is observed for complex **1**. At 4 K, a broad signal ($\Delta H = 1500$ G) is observed with a weak signal at low field. As the temperature rises, the low-field signals increase in relative intensity. This temperature dependence is roughly the opposite of that observed in complexes **2** and **3**, which is consistent with a reversal in the ordering of the lowest energy spin states between the complexes. The epr spectra for **4** and **5** are analogous, indicating an $S = {}^1/_2$ ground state, in agreement with the susceptibility and magnetization measurements. Finally, the epr spectra for **6** at 4 and 77 K are shown in Figure 9. At 4 K, the system is highly complex but, evidently, the signals at low fields indicate strong anisotropy due to $m_s =$

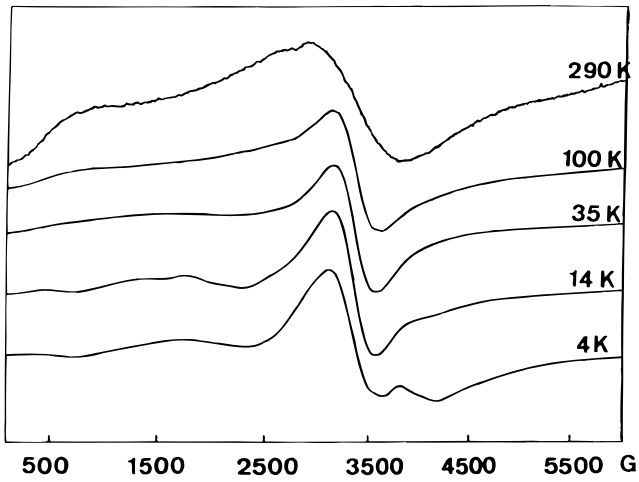

Figure 8. Temperature dependence of the X-band epr spectra of a powdered sample of $[Mn_3O(2F\text{-benzoato})_6(pyr)_3]$ (**1**) (spin ground state $^1/_2$).

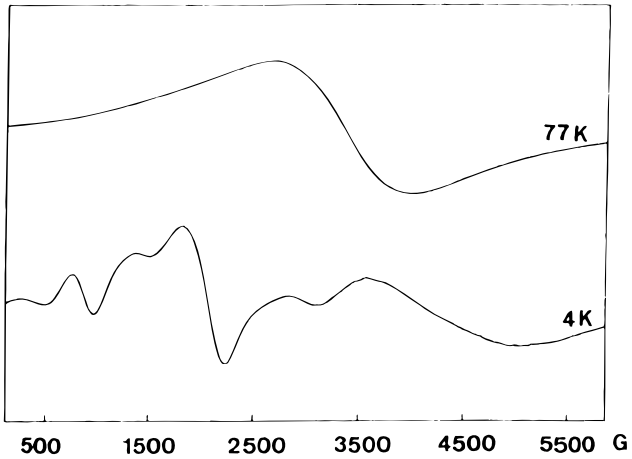

Figure 9. Temperature dependence of the X-band epr spectra of a powdered sample of $[Mn_3O(3Br\text{-benzoato})_6(pyr)_2(H_2O)]\cdot{}^1/_4H_2O$ (**6**) (spin ground state intermediate between $^3/_2$ and $^1/_2$).

$\pm^1/_2$ for $S = {}^3/_2$ ground state. At 77 K, there is only a broad signal centered at $g \approx 2$. Thus, the epr spectra provide proof that the spin ground state at low temperature is not a pure $S = {}^1/_2$ but is mixed with the $S = {}^3/_2$ state, in accordance with the susceptibility and magnetization measurements.

Variability of the Ground State. Influence of the Ligands. It has been demonstrated elsewhere[2] that the acetato trinuclear analogue has a $S = {}^3/_2$ ground state. Its molecular structure contains three pyridine terminal ligands. In contrast, the analogous trinuclear complex with benzoate, which has two pyridine and one water molecules as terminal ligands, has a ground state of $S = {}^1/_2$: thus, upon substitution of H_2O for pyridine ligation on the Mn^{II} ions, the spin of the ground state has changed from $^3/_2$ to $^1/_2$. In the complexes presented in this paper, **1** has three pyridine terminal ligands but the ground state is clearly $^1/_2$; **2** and **3** also have three pyridine terminal ligands according to their elemental analyses. We were not able to obtain a well-formed single crystal of **3**, but for **2,** it was possible to solve the structure of a poorly diffracting single crystal, and although it was not possible to determine precise angles and distances, we could confirm that there were three pyridine groups as terminal ligands. The complex **3** has similar IR as complex **2**, and the results of elemental analysis are consistent with three pyridine as terminal ligands. Complexes **4**, **5**, and **6** have two pyridine molecules and one water molecule, according to their analysis and crystal structure (**5**, **6**): thus a ground state of $^1/_2$ would not be surprising, in agreement with the benzoato analogue.[2] This is true for **4** and **5** but not for **6**, whose ground state is a thermal admixture of closely spaced $^1/_2$ and $^3/_2$. Thus, new and complementary results arise when trying to interpret the relationship between the structure and magnetism of **1** and **6**. **1** shows a $S = {}^1/_2$ ground state although it has three pyridines as terminal ligands; **6** is an intermediate case betweeen $^1/_2$ and $^3/_2$ ground states although it is isostructural with **5**, which clearly has a $S = {}^1/_2$ ground state. This indicates that the influence of the ligands (already pointed out elsewhere[2]) is of considerable importance, not only magnetically but also crystallographically. From the latter perspective, the 2-halobenzoic acids lead to the presence of three pyridine molecules as terminal ligands and the 3-halobenzoic acids lead to the presence of two pyridine and one H_2O molecules as terminal ligands. Magnetically speaking, all ligands are important: with three pyridine ligands the ground state is $^3/_2$ for **2** and **3** but $^1/_2$ for **1**; with two pyridine and one H_2O the ground state is $^1/_2$ except for **6**, whose ground state is a thermal mixture between $^1/_2$ and $^3/_2$.

Acknowledgment. We are very grateful for the financial support given by the Dirección General de Investigación Científica y Técnica (Spain) (Grant PB93/0772); NATO Project CGR 93/0976, and the Swiss National Science Foundation (Grants 20.39132.93 and 20.45315.95). B.A. also acknowledges the F.P.I. Grant from the Ministerio de Educación y Ciencia (Spain).

Supporting Information Available: Tables giving crystal data and details of the structure determination, anisotropic thermal parameters, bond angles and distances, and hydrogen atom coordinates for **1**, **5**, and **6** (30 pages). Ordering information is given on any current masthead page.

IC961252X